

# Merlin: Multi-View Representation Learning for Robust Multivariate Time Series Forecasting with Unfixed Missing Rates

Chengqing Yu

Fei Wang\*

Institute of Computing Technology,  
Chinese Academy of Sciences  
State Key Laboratory of AI Safety  
University of Chinese Academy of Sciences,  
Beijing, China  
[{yuchengqing22b,wangfei,19b}@ict.ac.cn](mailto:{yuchengqing22b,wangfei,19b}@ict.ac.cn)

Wei Wei

School of Computer Science and Technology,  
Huazhong University of Science and Technology,  
Wuhan, China  
[weiw@hust.edu.cn](mailto:weiw@hust.edu.cn)

Chuanguang Yang

Zezhi Shao

Tao Sun

Tangwen Qian

Institute of Computing Technology,  
Chinese Academy of Sciences  
State Key Laboratory of AI Safety, Beijing, China  
[{yangchuanguang,shaozezhi,suntao,qiantangwen}@ict.ac.cn](mailto:{yangchuanguang,shaozezhi,suntao,qiantangwen}@ict.ac.cn)

Zhulin An

Yongjun Xu\*

Institute of Computing Technology,  
Chinese Academy of Sciences  
State Key Laboratory of AI Safety  
University of Chinese Academy of Sciences,  
Beijing, China  
[{anzhulin,xyj}@ict.ac.cn](mailto:{anzhulin,xyj}@ict.ac.cn)

preserving forecasting accuracy. Experiments on four real-world datasets demonstrate the superiority of Merlin.

## CCS Concepts

- Information systems → Data mining.

## Keywords

Multivariate Time Series Forecasting with Unfixed Missing Rates, Multi-View Representation Learning, Offline Knowledge Distillation, Multi-View Contrastive Learning

## ACM Reference Format:

Chengqing Yu, Fei Wang, Chuanguang Yang, Zezhi Shao, Tao Sun, Tangwen Qian, Wei Wei, Zhulin An, and Yongjun Xu. 2025. Merlin: Multi-View Representation Learning for Robust Multivariate Time Series Forecasting with Unfixed Missing Rates. In *Proceedings of the 31st ACM SIGKDD Conference on Knowledge Discovery and Data Mining V.2 (KDD '25), August 3–7, 2025, Toronto, ON, Canada*. ACM, New York, NY, USA, 12 pages. <https://doi.org/10.1145/3711896.3737046>

## KDD Availability Link:

The source code of this paper has been made publicly available at <https://doi.org/10.5281/zenodo.15508818>.

## 1 Introduction

Multivariate Time Series Forecasting (MTSF) widely exists in transportation, environment, weather and other areas [17, 22, 41, 50]. It consists of multiple numerical sequences that change over time, which typically contain global information (such as periodicity and trends) and local information (such as detailed changes) along the temporal dimension [47, 56]. These global and local information constitute the semantics of time series, and fully mining these semantics is crucial for achieving accurate forecasting [19, 39].

\*Fei Wang and Yongjun Xu are the corresponding authors.



This work is licensed under a Creative Commons Attribution 4.0 International License.  
KDD '25, Toronto, ON, Canada  
© 2025 Copyright held by the owner/author(s).  
ACM ISBN 979-8-4007-1454-2/2025/08  
<https://doi.org/10.1145/3711896.3737046>

Deep learning-based models, such as Spatial-Temporal Graph Neural Networks (STGNNs) [44, 45] and Transformers [10, 65], can fully mine semantics from MTS, but they generally require complete observations to maintain accurate forecasting [66]. In reality, due to factors such as natural disasters and component failures, data collectors can easily malfunction and fail to output data normally [73]. In this case, existing models only use incomplete observations to predict future values, limiting their performance [12]. To illustrate, we evaluate the performance of several models [43, 57] under different missing rates on the PEMS04 dataset. As shown in Figure 1(a), the forecasting errors (Mean Absolute Error) of these models increase significantly as the missing rate increases.

To mitigate the adverse effects of incomplete MTS data, we delve deeper into a question: **how do missing values lead to the performance degradation of these models?** We find that a large number of missing values<sup>1</sup> in historical observations can severely disrupt the semantics of MTS, while existing models exhibit poor robustness in this scenario. As shown in Figure 1 (b), missing values disrupt the global information (such as periodicity) and introduce abnormal local information such as sudden changes (from normal to zero) and abnormal straight lines. Existing models easily capture these anomalies instead of the original semantics, leading to a degradation in performance. Besides, the distribution of missing values may change over time, leading to unfixed missing rates across different time periods. If existing models [43, 57] do not train separate models for each missing rate, their performance will significantly decline, exhibiting poor robustness to unfixed missing rates.

An intuitive solution to enhancing the performance of forecasting models is to use imputation methods to recover missing values and propose two-stage or end-to-end modeling approaches [48, 49, 67]. However, these methods face two challenges: (1) existing imputation methods [1, 35, 54] usually require reconstructing both missing and normal values, which disrupts the local information and leads to error accumulation; (2) when dealing with unfixed missing rates, existing imputation methods [20, 34, 74] require training separate models for different missing rates to ensure data recovery accuracy. When imputation and forecasting models do not train separate models for each missing rate, their forecasting performance significantly declines, exhibiting poor robustness when dealing with unfixed missing rates.

To solve the above problems and achieve robust MTSF with unfixed missing rates, we believe that the key idea is to enhance the capability of forecasting models for semantic alignment, which includes **two objectives**: (1) complete observations have more accurate global and local information, and we need to help forecasting models mine similar semantics from incomplete observations; (2) different missing rates have varying impacts on the original semantics of MTS, and we need to help forecasting models align the semantics as much as possible between different missing rates. To this end, we propose Multi-View Representation Learning (Merlin), taking advantage of offline knowledge distillation (KD) and multi-view contrastive learning (CL). **For objective 1**, based on the idea of offline knowledge distillation, we first train a teacher model using complete observations and then use the same architecture to obtain a student model, which is trained on incomplete observations.

<sup>1</sup>Missing values in most datasets, such as PEMS04, are typically treated as zeros.

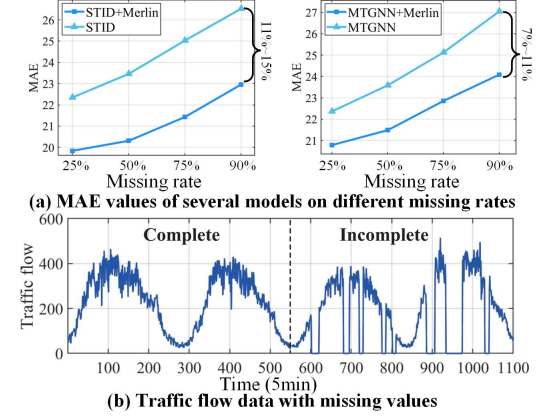


**Figure 1: Examples of MTSF with missing values on PEMS04.**  
**(a)** Although the forecasting errors of existing models increase significantly as the missing rate increases, Merlin can reduce their forecasting errors.  
**(b)** Missing values disrupt the global information and bring abnormal local information. The missing rates are unfixed across different time periods.

When training the student model, we input complete observations into the teacher model and transfer the generated representations and forecasting results as knowledge to constrain the student model. This ensures that the representations and forecasting results generated by the student model from incomplete observations are as similar as possible to those generated by the teacher model (the loss between them is as small as possible). In this way, the student model can mine semantics from incomplete observations that approximate those obtained from complete observations. **For objective 2**, based on the idea of multi-view contrastive learning, we first treat incomplete observations from the same time point but with different missing rates as positive data pairs, and those from different time points as negative data pairs. Then, we propose a contrastive loss as a constraint for the student model to enhance the dissimilarity of negative data pairs and the similarity of positive data pairs. Through this approach, the student model can align the semantics between incomplete observations with different missing rates, without the need to train several separate models for different missing rates. As shown in Figure 1 (a), Merlin can significantly enhance the robustness of existing models to unfixed missing rates and improve their forecasting performance. **The main contributions can be outlined as follows:**

- The existing models encounter robustness issues when dealing with unfixed missing rates, including two phenomena: (1) missing values significantly disrupt the semantics (global and local information) of MTS; (2) the missing rate typically changes over time, and existing models require training separate models for different missing rates.
- The key idea to achieving robust MTSF with unfixed missing rates is to help existing models achieve semantic alignment between incomplete observations with different missing rates and complete observations. To this end, we propose Merlin based on offline knowledge distillation and multi-view contrastive learning.

- We design experiments on four real-world datasets. Results show that Merlin can enhance the performance of existing models more effectively than imputation methods. Besides, with the help of Merlin, existing models only need to be trained once to adapt to unfixed missing rates.

## 2 Related Work

### 2.1 Time Series Analysis with Missing Values

Existing works typically design imputation methods or end-to-end forecasting models to address the negative impact of missing values on MTSF [67]. Since data collectors typically function properly during the early stages of deployment, and missing values occur gradually after a period of time, existing works generally assume that data collectors can collect complete data (complete observations) during the training phase [12, 33]. Under this assumption, in the training phase, existing works first mask complete observations to generate incomplete observations with different missing rates. Then, they use complete observations as labels and combine reconstruction loss to train imputation methods or end-to-end models [3, 60]. In the test phase, they only use incomplete observations to evaluate the performance of several models.

Based on the above assumptions, in terms of both technology and scenario, end-to-end forecasting models [8, 48] first convert complete observations into incomplete observations based on random point missing. Then, they propose additional components (such as reconstruction loss or GNN) to directly model incomplete observations for each missing rate and achieve forecasting. Imputation methods [7, 20, 34] also train separate models for each missing rate to restore incomplete observations, using reconstruction loss and data recovery components (such as variant attention or GNN).

In summary, mainstream works require training separate models for each missing rate, assuming that the data is complete during the training phase, and are typically conducted under the random point missing scenario. To be fair, we primarily conduct experiments and evaluate baselines based on the above scenario, assumptions, and settings. However, considering more realistic scenarios, we analyze other data missing scenarios in Section 4.6 and evaluate the performance of existing works when the training sets contain missing values in Appendix B.

### 2.2 Time Series Forecasting Models

Classic STGNNs [15, 26, 31, 58] combine the Graph Convolutional Network (GCN) and sequence models to realize MTSF. At present, existing state-of-the-art (SOTA) STGNNs [25, 64] introduce graph learning to further improve their forecasting performance. Different from STGNNs, Transformer-based models [55, 68, 72] combine temporal attention and spatial attention, or their variants, to improve forecasting results. However, these complex models suffer from high complexity and limited scalability [4, 69]. Currently, light-weight models based on Multi-Layer Perceptron (MLP) have gained widespread recognition. Chen et al. [5] propose TSMixer, which uses all-MLP architecture to realize MTSF. Shao et al. [43] analyze the core of modeling MTS and propose an MLP framework based on the Spatial-Temporal Identity (STID). In summary, a suitable MLP framework can achieve satisfactory results more efficiently

than complex models. Considering that STID analyzes the characteristics of MTSF and performs satisfactorily on most datasets, it is selected as the backbone in this paper. In addition to STID, we also evaluate the performance improvement of Merlin on other backbones (STGNNs and Transformer) in Section 4.3.

### 2.3 Knowledge distillation

Knowledge distillation can transfer valuable knowledge from the teacher model to the student model to improve the student model's performance [59]. Mainstream techniques include offline knowledge distillation and online knowledge distillation. Among them, offline knowledge distillation offers advantages such as good stability, high flexibility, and a simplified training process. It improves the ability of the student model by continually guiding it to align with the teacher model [51, 63]. Huang et al. [23] use knowledge distillation to help the student model achieve semantic alignment between low-resolution and high-resolution data. Even when the input size is reduced by 50%, the student model can still maintain good performance. Monti et al. [36] propose a trajectory forecasting model based on knowledge distillation and spatial-temporal Transformer, enabling the student model to perform well with only 25% of historical observations. In summary, knowledge distillation helps the student model achieve satisfactory forecasting results when the effective information in the inputs is significantly reduced, thereby enhancing its robustness to missing values.

### 2.4 Contrastive learning

Multi-view contrastive learning enhances the model's ability to align the semantics of similar samples across different views [13, 14, 16, 28]. Woo et al. [53] treat the seasonal and trend components of MTS as different views and use contrastive learning to align their semantics. Yue et al. [70] propose hierarchical contrastive learning to help the model improve their ability to align the semantics of MTS with different scales. Dong et al. [19] combine different masking ways with contrastive learning to realize time series forecasting. Results show that contrastive learning can align the semantics of different masked time series and enhance the forecasting effect. Overall, contrastive learning can enhance the model's ability to distinguish negative data pairs and align the semantics between positive data pairs [30]. Therefore, if we effectively construct positive data pairs, contrastive learning can align the semantics of incomplete observations with different missing rates.

## 3 Methodology

### 3.1 Preliminaries

**Multivariate time series forecasting** [11]. Given a historical observation tensor  $X \in \mathbb{R}^{N_v \times N_H \times N_c}$  from  $N_H$  time slices in history, the model can predict the value  $Y \in \mathbb{R}^{N_v \times N_L}$  of the nearest. The core goal of MTSF is to construct a mapping function between the input  $X \in \mathbb{R}^{N_v \times N_H \times N_c}$  and output  $Y \in \mathbb{R}^{N_v \times N_L}$ .  $N_v$  is the number of sequences.  $N_H$  is the historical length.  $N_L$  is the future length.  $N_c$  is the number of features.

**Multivariate time series forecasting with missing values** [46]. In this task, we need to mask  $M\%$  point randomly from the historical observation tensor  $X \in \mathbb{R}^{N_v \times N_H \times N_c}$ . After the above processing, a new input feature  $X_M \in \mathbb{R}^{N_v \times N_H \times N_c}$  is obtained. The

core goal of this task is to construct a mapping function between the input  $X_M \in \mathbb{R}^{N_v \times N_H \times N_c}$  and output  $Y \in \mathbb{R}^{N_v \times N_L}$ .

**Offline knowledge distillation** [18, 62]. It can transfer valuable knowledge from the teacher model to the student model as an additional loss function, thereby constraining the student model's modeling process and improving its performance. When training the student, the teacher model does not need to update its parameters, and the teacher model is not used during test.

**Contrastive learning** [61, 71]. Its main goal is to introduce contrastive loss to help the model enhance the dissimilarity of negative data pairs and the similarity of positive data pairs, thereby fully extracting invariant information from positive data pairs. Therefore, it can effectively improve the model's generalization.

### 3.2 Overall Framework

The overall framework is shown in Figure 2. We use STID as the backbone and propose Merlin, which combines offline knowledge distillation with multi-view contrastive learning and is used to train STID. A basic introduction to STID is provided in Section 3.3.

During the training phase, we follow the assumption of existing works that the training sets are complete, as discussed in Section 2.1. Based on offline knowledge distillation, we first use complete observations to train the teacher model. Then, when using incomplete observations to train the student model, we transfer the representations and forecasting results generated by the teacher model as knowledge, providing constraints (MSE loss) for the student model. Meanwhile, for the representations obtained by the student model when encoding incomplete observations with different missing rates, we propose a contrastive loss based on multi-view contrastive learning to further constrain the student model to align the semantics between them. The MSE loss from knowledge distillation and the contrastive loss constitute the key components of Merlin, helping STID achieve semantic alignment between incomplete observations and complete observations. A detailed introduction to knowledge distillation and contrastive learning can be found in Section 3.4 and Section 3.5, respectively.

During the test phase, the student model directly uses incomplete observations with different missing rates for forecasting, without the need for the teacher model. Compared to existing works, the use of data in both the training and test phases remains fair and reasonable. Although most related works assume that training sets are complete, training sets in the real world may contain missing values, which affects the performance of the teacher or imputation models. Therefore, in Appendix B, we analyze the performance of Merlin when the training sets contain missing values.

### 3.3 Backbone

In this section, we briefly introduce the basic structure of the backbone (STID), which is composed of a embedding layer,  $L$  fully connected (FC) layer and a regression layer. The detailed description and definition of STID can be found in the reference [43]. The basic modeling process of STID is shown as follows:

Step I: First, the embedding layer based on a FC layer is used to transform the input feature  $X$  into a hidden representation  $H$ :

$$H = \text{FC}(X), \quad (1)$$

where,  $\text{FC}(\cdot)$  is the fully connected layer.

Step II: Then, the spatial-temporal identity embeddings ( $S_E$ ,  $T_E^D$  and  $T_E^W$ ) are passed to  $H$  as additional inputs to the encoder, helping the model capture spatial-temporal correlations.

$$H_E = \text{Concat}(H, S_E, T_E^D, T_E^W), \quad (2)$$

where,  $\text{Concat}(\cdot)$  means concatenate several tensors. Assuming  $N_v$  time series and  $N_H$  time slots in a day and  $N_w = 7$  days in a week.  $S_E \in \mathbb{R}^{N_v \times D}$  is the spatial identity embedding.  $T_E^D \in \mathbb{R}^{N_H \times D}$  and  $T_E^W \in \mathbb{R}^{N_w \times D}$  are temporal embedding.  $D$  is the embedding size.

Step III: The encoder based on  $L$  layers of MLP with the residual connection is used to mine the above representation  $Z$ . The  $l$ -th MLP layer can be denoted as:

$$H_E^{l+1} = \text{FC}(\text{Relu}(\text{FC}(H_E^l))) + H_E^l, \quad (3)$$

where,  $\text{Relu}(\cdot)$  is the activation function.

Step IV: Finally, based on the hidden representation  $H_E^L$ , the regression layer is used to obtain the forecasting results  $Y$ .

$$Y = \text{FC}(H_E^L). \quad (4)$$

Compared to complex models, STID has two main advantages: (1) It introduces spatial-temporal identity embeddings to provide the model with additional global information, effectively mitigating the damage of missing values. (2) Based on the above embeddings, STID can effectively model MTS with the computational complexity of  $O(N_H)$ . Next, we show how to use hidden representations  $H_E^L$  and forecasting results  $Y$  for offline knowledge distillation with multi-view contrastive learning.

### 3.4 Offline Knowledge Distillation

We use two STID models as the student model and the teacher model. The inputs to the teacher model are complete observations  $X$ . It produces hidden representations  $H_{E, \text{Teacher}}^L$  and forecasting results  $Y_{\text{Teacher}}$ . The inputs to the student model are incomplete observations  $X_{M,1}$  to  $X_{M,m}$ .  $m$  stands for the number of missing rates. It produces  $m$  hidden representations  $H_{E,1}^L$  to  $H_{E,m}^L$  and  $m$  forecasting results  $Y_{M,1}$  to  $Y_{M,m}$ . The offline knowledge distillation consists of two components: the hidden representation distillation and the forecasting result distillation.

**Hidden representation distillation:** It refers to transferring the representations produced by the teacher model to the student model, aiming to minimize the mean squared error (MSE) between the representations produced by the student model and those produced by the teacher model. Its specific formula is shown as follows:

$$L_{HD} = \sum_{i=1}^m \text{Mean}((H_{E, \text{Teacher}}^L - H_{E,i}^L)^2), \quad (5)$$

where,  $\text{Mean}(\cdot)$  is the mean of the Tensor.

**Forecasting result distillation:** It refers to transferring the forecasting results produced by the teacher model to the student model, with the objective of minimizing the MSE between the forecasting results produced by the student model and those produced by the teacher model. The specific formula is shown as follows:

$$L_{RD} = \sum_{i=1}^m \text{Mean}((Y_{\text{Teacher}} - Y_{M,i})^2). \quad (6)$$

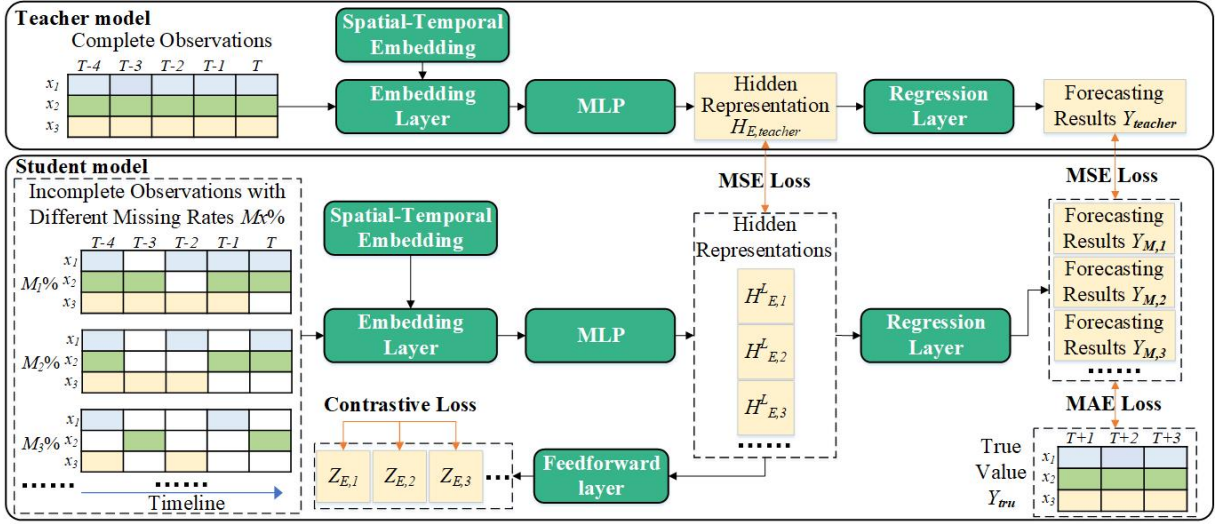


Figure 2: The overall framework of our model. During the training phase, we first mask the raw data (complete observations) to obtain multiple new data with different missing rates (incomplete observations). The complete observations are used to train the teacher model, and the incomplete observations are used to train the student model. The teacher model guides the student model to align the semantics between complete and incomplete observations. Contrastive loss enhances the student model’s robustness to incomplete observations with different missing rates. During the test phase, the trained student model is used to directly process incomplete observations and obtain forecasting results, without the use of the teacher model.

Based on  $L_{HD}$  and  $L_{RD}$ , the teacher model can guide the student model to use incomplete observations to generate representations and forecasting results similar to those generated by the teacher model. In this way, the student model can achieve semantic alignment between incomplete observations and complete observations.

### 3.5 Multi-View Contrastive Learning

The missing rates are usually unfixed at different time periods. To further enhance the robustness of the student model and realize the semantic alignment between incomplete observations with different missing rates, we propose multi-view contrastive learning. We use incomplete observations with different missing rates at the same time point as positive data pairs, and use incomplete observations at different time point (other samples within a batch) as negative data pairs. For representations  $H_{E,1}^L$  to  $H_{E,m}^L$  encoded by incomplete observations with different missing rates, we achieve multi-view contrastive learning using the pairwise contrastive learning method. The specific steps are shown as follows:

Step I: Considering that appropriate dimension reduction can enhance the effectiveness of contrastive learning, we use an FC layer to reduce the dimension of the hidden representations  $H_{E,1}^L$  to  $H_{E,m}^L$ , and obtain the representations  $Z_{E,1}$  to  $Z_{E,m}$ .

$$Z_{E,1} = \text{FC}(H_{E,1}^L). \quad (7)$$

Step II: We use the  $Z_{E,1}$  and  $Z_{E,2}$  to obtain  $2N_s$  samples. In  $Z_{E,1}$  and  $Z_{E,2}$ , the corresponding two samples form a positive data pair, while the other samples are their negative data pairs. Based on cross-entropy loss, the contrast loss between any two samples  $z_{E,i}$

and  $z_{E,j}$  is calculated using the following formula:

$$l_{i,j} = -\log\left(\frac{\exp(\text{sim}(z_{E,i}, z_{E,j})/\tau)}{\sum_{k=1 \& k \neq i}^{2N_s} \exp(\text{sim}(z_{E,i}, z_{E,k})/\tau)}\right), \quad (8)$$

where,  $\exp(\cdot)$  is the exp function.  $\text{sim}(\cdot)$  is the Cosine similarity.  $N_s$  is the number of samples.  $\tau$  is the temperature parameter.

Step III: Based on the above formula, we calculate the contrastive loss for all samples between  $Z_{E,1}$  and  $Z_{E,2}$ , and obtain  $L_{Z1,Z2}$ .

$$L_{Z1,Z2} = \frac{1}{2N_s} \sum_{k=1}^{N_s} (l_{2k-1,2k} + l_{2k,2k-1}). \quad (9)$$

Step IV: The final multi-view contrastive learning loss  $L_{CL}$  is obtained by computing the pairwise contrastive losses from  $Z_{E,1}$  to  $Z_{E,m}$ .

$$L_{CL} = \frac{2}{m(m-1)} \left( \sum_{Zj=Zi}^m \sum_{Zi=1}^{m-1} L_{Zi,Zj} \right). \quad (10)$$

### 3.6 Loss Function

Since MTSF is a regression task, we also need to carry out the supervised learning process. To this end, we also incorporate the ground truth and L1 loss [2] to train the student model.

$$L_{Pre} = \sum_{i=1}^m \text{Mean}(|Y_{tru} - Y_{M,i}|), \quad (11)$$

where,  $Y_{tru}$  is the ground truth.  $|\cdot|$  stands for absolute value.

Finally, we need to effectively combine all the above loss functions. In this paper, we use the method of adding all loss functions, which can avoid the problem of information forgetting [21]. The final loss  $L_{Finally}$  function is shown as follows:

**Table 1: The statistics of four datasets.**

Datasets	Variates	Timesteps	Granularity
METR-LA	207	34272	5 minutes
PEMS04	307	16992	5 minutes
China AQI	1300	41506	1 hour
Global Wind	2908	10957	1 day

$$L_{Finally} = \beta_1 * L_{Pre} + \beta_2 * (L_{HD} + L_{RD}) + \beta_3 * L_{CL}, \quad (12)$$

where,  $\beta$  stands for the weight of the loss.  $\beta_2$  and  $\beta_3$  need to be divided by the current epoch size in each epoch. After completing the process of the training phase, the test phase is performed by using only the student model, without using the teacher model.

## 4 Experiment and Analysis

### 4.1 Experimental Design

**Datasets.** We select four real-world datasets from different domains: METR-LA<sup>2</sup>, PEMS04<sup>3</sup>, China AQI<sup>4</sup>, and Global Wind<sup>5</sup>. The basic statistics for these datasets are shown in Table 1.

**Baselines.** We select baselines from three perspectives: (1) Three SOTA one-stage forecasting models: TSMixer [5], FourierGNN [64], and DSformer [68]. (2) To demonstrate the improvement of Merlin on STID, we compare the STID+Merlin with the raw STID. Besides, we combine four imputation methods with STID to obtain multiple two-stage models: STID+GATGPT [9], STID+SPIN [34], STID+GPT2 [74] and STID+TI-MAE [27]. (3) We combine existing multivariate time series forecasting models with imputation models, and obtain several two-stage models as baselines: iTransformer [32] + TimesNet [54], MTGNN [57] + SPIN, TimeMixer[52] + GATGPT, and DUET[40] + GPT2. The previous method for each combination is the forecasting model.

**Setting.** We design the experiments from the following aspects: (1) According to ratios in [38, 42], four datasets are uniformly divided into training sets, validation sets, and testing sets. (2) The history length and future length are 12. All metrics are calculated as the average of the 12-step forecasting results. (3) We randomly assign mask points with ratios of 25%, 50%, 75%, and 90%. The value of the masked point is uniformly set to zero. Experiments are repeated with 5 different random seeds for each model. The final metrics are calculated as the mean value of repeated experiments. (4) To prove the robustness of Merlin, we train it once, using data with multiple missing rates. Specifically, the student model is trained simultaneously using data with missing rates of 25%, 50%, 75%, and 90%. (5) Our code is available at this link<sup>6</sup>.

**Metrics.** Three classical metrics are used, including MAE (Mean Absolute Error), RMSE (Root Mean Square Error) and MAPE (Mean Absolute Percentage Error) [29]. The smaller these metrics are, the lower the forecasting errors.

<sup>2</sup><https://github.com/liyaguang/DCRNN>

<sup>3</sup><https://github.com/guoshnBJTU/ASTGNN/tree/main/data>

<sup>4</sup><https://quotsoft.net/air/>

<sup>5</sup><https://www.ncei.noaa.gov/>

<sup>6</sup><https://github.com/ChengqingYu/Merlin>

### 4.2 Main Results

Table 2 shows the performance comparison results of all baselines and Merlin. We can draw the following conclusions: (1) Compared with two-stage models, the forecasting errors of all single-stage models are larger. The main reason is that existing single-stage models are not robust to incomplete observations. (2) Compared with imputation methods, Merlin improves the forecasting performance of STID more effectively. The main reason is that Merlin effectively combines the advantages of multi-view contrastive learning and offline knowledge distillation, which can significantly enhance the robustness of STID in modeling incomplete observations. (3) STID+Merlin works better than all baselines in all cases. Firstly, we select the high-performance STID as our backbone model, which introduces spatial-temporal embeddings to provide additional global information for the model, helping to mitigate the impact of missing values. Secondly, we introduce offline knowledge distillation to guide STID on how to align the semantics between incomplete observations and complete observations, thereby enhancing STID’s robustness to incomplete observations. Finally, we propose multi-view contrastive learning to achieve semantic alignment between incomplete observations with different missing rates, further improving its robustness. Therefore, STID+Merlin can achieve the best forecasting results on all datasets and all missing rates. In the next section, we will further evaluate Merlin’s performance improvement effects on other backbones.

### 4.3 Transferability of Merlin

To validate the effectiveness and transferability of Merlin, we choose three other models (TimeMixer, DUET, and MTGNN) as backbones and compare the performance of Merlin with other imputation methods (GATGPT, GPT2, TI-MAE and SPIN). Table 3 shows the MAE values of Merlin and other imputation methods. We can draw the following conclusions: (1) One-stage models struggle to perform well. Specifically, missing values make it difficult for existing models to fully mine semantics from incomplete observations, resulting in unsatisfactory results. (2) Compared with imputation methods, Merlin can better restore the performance of all backbone models. The experimental results fully prove the transfer ability and practical value of Merlin, which can effectively enhance the robustness of all backbones.

### 4.4 Ablation Experiments

We conduct ablation experiments from the following four perspectives: (1) **w/o HD**: We remove the hidden representation distillation. (2) **w/o RD**: We remove the forecasting result distillation. (3) **w/o KD**: We removed the teacher model and knowledge distillation. In this case, STID achieves contrastive learning using both complete and incomplete observations. (4) **w/o CL**: We remove the multi-view contrastive learning.

Figure 3 shows the results of the ablation experiment. We can draw the following conclusions: (1) The forecasting result distillation has the least effect on the results. It shows that as long as the encoder can fully mine semantics from MTS, the decoder can realize effective forecasting. (2) When either the hidden representation distillation or the contrastive learning is removed individually, the model performance drops significantly. This is mainly because both

**Table 2: Performance comparison results of several models. The best results are shown in bold.**

Datasets	Models	Missing rate 25%			Missing rate 50%			Missing rate 75%			Missing rate 90%		
		MAE	MAPE	RMSE									
METR-LA	DSformer	3.44	10.45	7.21	3.61	11.15	7.52	3.82	12.31	8.11	4.05	13.57	8.84
	FourierGNN	3.42	10.39	7.17	3.59	10.96	7.47	3.78	12.18	7.95	3.97	12.89	8.62
	TSMixer	3.45	10.48	7.25	3.60	11.09	7.53	3.84	12.34	8.21	4.01	13.42	8.76
	iTransformer+TimesNet	3.37	10.31	7.02	3.51	10.77	7.39	3.72	11.61	7.81	3.89	12.47	8.35
	MTGNN+SPIN	3.26	9.79	6.73	3.45	10.45	7.18	3.59	10.97	7.56	3.84	12.31	8.24
	TimeMixer+GATGPT	3.35	9.97	6.91	3.49	10.65	7.27	3.63	11.23	7.59	3.86	12.29	8.28
	DUET+GPT2	3.32	9.95	6.87	3.48	10.62	7.26	3.61	11.18	7.54	3.87	12.42	8.31
	STID (Raw)	3.39	10.27	7.05	3.53	10.88	7.45	3.75	11.83	7.86	3.92	12.59	8.43
	STID+SPIN	3.28	9.84	6.79	3.44	10.39	7.20	3.60	11.06	7.55	3.78	12.02	7.93
PEMS04	STID+GPT2	3.31	9.91	6.83	3.43	10.44	7.18	3.55	10.85	7.49	3.75	11.84	7.86
	STID+TI-MAE	3.34	9.92	6.88	3.46	10.51	7.22	3.58	10.93	7.52	3.76	11.85	7.89
	STID+GATGPT	3.27	9.85	6.75	3.39	10.35	7.06	3.52	10.87	7.43	3.73	11.76	7.85
	STID+Merlin	<b>3.21</b>	<b>9.41</b>	<b>6.64</b>	<b>3.28</b>	<b>9.85</b>	<b>6.78</b>	<b>3.43</b>	<b>10.42</b>	<b>7.18</b>	<b>3.65</b>	<b>11.25</b>	<b>7.64</b>
	DSformer	23.65	16.24	38.34	24.37	16.29	39.83	25.87	17.66	41.73	27.43	18.41	43.17
	FourierGNN	22.95	15.42	37.06	24.06	16.15	39.48	25.69	17.49	41.48	27.29	18.32	42.81
	TSMixer	23.37	15.81	37.40	24.26	16.04	39.57	25.76	17.54	41.65	28.04	18.58	43.49
	iTransformer+TimesNet	21.64	15.08	34.56	22.75	15.34	36.57	24.18	16.06	39.42	25.57	17.56	41.23
	MTGNN+SPIN	20.94	14.71	33.52	21.78	15.07	35.22	23.36	15.78	37.64	24.92	16.63	40.77
China AQI	TimeMixer+GATGPT	21.38	14.87	34.42	22.42	15.13	36.03	23.98	15.94	39.23	25.43	17.56	41.10
	DUET+GPT2	21.29	14.84	34.37	22.51	15.21	36.23	24.16	16.02	39.54	25.25	17.34	40.89
	STID (Raw)	22.35	15.08	36.05	23.46	16.18	37.92	25.03	17.13	40.87	26.53	17.91	42.32
	STID+SPIN	20.47	14.22	32.64	21.69	15.02	34.97	23.26	15.57	37.29	24.79	16.52	40.58
	STID+GPT2	20.76	14.36	32.96	21.63	14.92	34.67	23.15	15.51	37.21	24.51	16.37	40.16
	STID+TI-MAE	20.81	14.52	33.27	21.75	15.05	35.04	23.04	15.42	37.15	24.34	16.32	39.77
	STID+GATGPT	20.42	14.15	32.58	21.36	14.83	34.12	22.87	15.26	36.94	24.09	15.94	39.36
	STID+Merlin	<b>19.84</b>	<b>13.85</b>	<b>31.65</b>	<b>20.31</b>	<b>14.07</b>	<b>32.37</b>	<b>21.43</b>	<b>14.95</b>	<b>34.45</b>	<b>22.96</b>	<b>15.56</b>	<b>37.07</b>
	DSformer	17.52	35.36	29.81	19.32	39.27	31.74	20.47	43.66	33.85	23.48	45.52	38.69
Global Wind	FourierGNN	17.35	35.25	29.27	19.14	38.43	31.29	20.96	43.83	34.04	24.06	46.25	39.43
	TSMixer	17.03	34.83	28.84	18.85	37.68	30.62	20.28	43.54	33.42	23.65	45.93	38.94
	iTransformer+TimesNet	16.49	32.06	28.07	17.79	35.76	29.45	20.03	42.76	32.98	23.04	45.65	37.68
	MTGNN+SPIN	15.83	31.89	27.21	16.97	34.13	28.79	18.91	40.56	30.77	22.18	44.92	36.03
	TimeMixer+GATGPT	16.09	32.56	27.48	17.39	34.82	29.04	19.86	41.37	32.27	22.57	45.36	36.81
	DUET+GPT2	15.97	32.04	27.35	17.04	34.73	28.91	19.34	40.85	31.84	22.30	45.01	36.39
	STID (Raw)	16.86	34.46	28.81	18.56	39.95	30.24	20.36	43.63	33.17	23.42	45.84	38.54
	STID+SPIN	15.39	30.25	26.64	16.83	34.67	28.69	18.43	40.43	30.06	21.86	44.78	35.83
	STID+GPT2	15.53	30.89	26.92	16.91	34.88	28.75	18.35	40.26	29.97	21.45	44.26	34.96
China AQI	STID+TI-MAE	15.74	31.72	27.09	17.08	35.24	28.97	18.29	40.07	29.82	21.58	44.53	35.23
	STID+GATGPT	15.46	30.53	26.87	16.67	34.34	28.43	18.14	39.96	29.65	21.07	43.79	34.36
	STID+Merlin	<b>15.21</b>	<b>30.42</b>	<b>26.38</b>	<b>15.84</b>	<b>32.06</b>	<b>27.25</b>	<b>17.43</b>	<b>35.68</b>	<b>29.34</b>	<b>20.18</b>	<b>43.36</b>	<b>33.31</b>
	DSformer	5.92	35.78	8.42	6.09	36.04	8.65	6.17	36.28	8.77	6.31	36.52	8.97
	FourierGNN	5.95	35.81	8.43	6.11	36.12	8.69	6.18	36.33	8.79	6.36	36.47	9.08
	TSMixer	5.93	35.75	8.39	6.07	35.94	8.62	6.21	36.12	8.84	6.33	36.34	9.02
	iTransformer+TimesNet	5.88	35.66	8.30	6.01	35.77	8.55	6.12	35.95	8.74	6.23	36.08	8.86
	MTGNN+SPIN	5.84	35.18	8.23	5.94	35.42	8.45	6.10	35.69	8.69	6.18	36.04	8.77
	TimeMixer+GATGPT	5.86	35.27	8.25	5.99	35.53	8.54	6.11	35.83	8.71	6.21	36.25	8.83
Global Wind	DUET+GPT2	5.85	35.38	8.29	5.95	35.54	8.52	6.09	35.72	8.65	6.17	35.94	8.75
	STID (Raw)	5.91	35.53	8.38	6.05	35.62	8.57	6.14	35.87	8.73	6.25	36.31	8.89
	STID+SPIN	5.80	34.57	8.25	5.94	35.18	8.41	6.12	35.41	8.69	6.21	36.27	8.82
	STID+GPT2	5.83	35.01	8.27	5.93	35.09	8.39	6.08	35.34	8.60	6.19	35.45	8.83
	STID+TI-MAE	5.84	35.06	8.28	5.94	35.15	8.43	6.09	35.26	8.62	6.18	35.41	8.76
	STID+GATGPT	5.82	34.75	8.26	5.91	34.92	8.37	6.07	35.08	8.57	6.15	35.34	8.73
	STID+Merlin	<b>5.76</b>	<b>34.28</b>	<b>8.17</b>	<b>5.85</b>	<b>34.59</b>	<b>8.32</b>	<b>5.97</b>	<b>34.83</b>	<b>8.49</b>	<b>6.08</b>	<b>35.04</b>	<b>8.64</b>

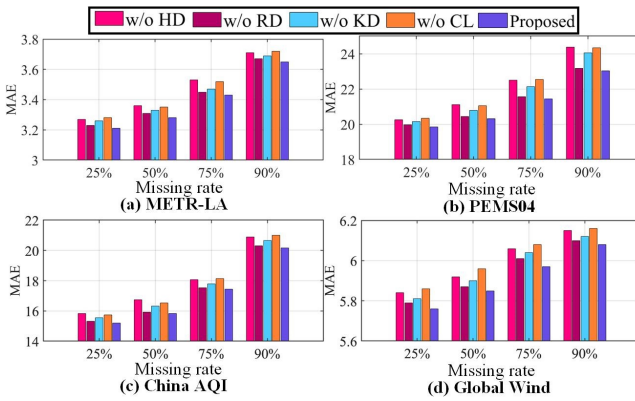
components play a critical role in achieving semantic alignment. (3) When contrastive learning is used without knowledge distillation, the model’s forecasting performance also declines, which further demonstrates the importance of knowledge distillation in aligning the semantics between complete and incomplete observations.

#### 4.5 Hyperparameter Analysis

Table 4 presents the main hyperparameters of Merlin and STID. We evaluate six hyperparameters that have the most significant impact on Merlin’s performance: Three weights of the loss ( $\beta_1$ ,  $\beta_2$  and  $\beta_3$ ), batch size, temperature parameter, and the dimensionality

**Table 3: MAE values of Merlin and other methods (The best results are shown in bold).**

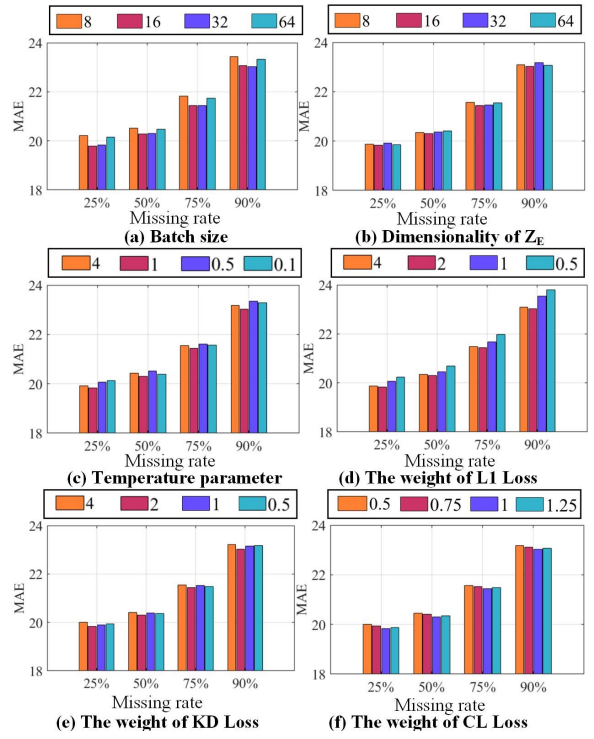
Backbone	Methods	METR-LA				Global Wind			
		25%	50%	75%	90%	25%	50%	75%	90%
DUET	+Merlin	<b>3.26</b>	<b>3.38</b>	<b>3.53</b>	<b>3.77</b>	<b>5.82</b>	<b>5.92</b>	<b>6.06</b>	<b>6.13</b>
	+GATGPT	3.28	3.45	3.56	3.83	5.83	5.94	6.08	6.15
	+GPT2	3.32	3.48	3.61	3.87	5.85	5.95	6.09	6.17
	+Ti-MAE	3.35	3.49	3.59	3.86	5.86	5.97	6.11	6.21
	+SPIN	3.29	3.51	3.64	3.91	5.83	5.96	6.12	6.25
	raw	3.41	3.56	3.79	3.95	5.93	6.07	6.15	6.29
TimeMixer	+Merlin	<b>3.31</b>	<b>3.42</b>	<b>3.57</b>	<b>3.81</b>	<b>5.83</b>	<b>5.95</b>	<b>6.08</b>	<b>6.17</b>
	+GATGPT	3.35	3.49	3.63	3.86	5.86	5.99	6.11	6.21
	+GPT2	3.39	3.54	3.67	3.89	5.87	6.02	6.13	6.23
	+Ti-MAE	3.41	3.55	3.71	3.95	5.91	6.03	6.12	6.24
	+SPIN	3.36	3.56	3.74	3.93	5.85	6.05	6.14	6.27
	raw	3.43	3.59	3.81	3.99	5.94	6.08	6.16	6.32
MTGNN	+Merlin	<b>3.24</b>	<b>3.37</b>	<b>3.52</b>	<b>3.75</b>	<b>5.81</b>	<b>5.93</b>	<b>6.04</b>	<b>6.11</b>
	+GATGPT	3.27	3.42	3.57	3.79	5.85	5.96	6.08	6.16
	+GPT2	3.31	3.43	3.61	3.85	5.87	5.97	6.11	6.19
	+Ti-MAE	3.33	3.46	3.64	3.87	5.88	5.99	6.13	6.21
	+SPIN	3.26	3.45	3.59	3.84	5.84	5.94	6.10	6.18
	raw	3.39	3.55	3.77	3.92	5.92	6.06	6.17	6.28

**Figure 3: Results of ablation experiments. w/o HD represents the removal of hidden representation distillation. w/o RD stands for the removal of forecasting result distillation. w/o KD indicates the deletion of the teacher model and the offline knowledge distillation. w/o CL represents the removal of multi-view contrastive learning.**

of  $Z_E$  [6]. The experimental results on PEMS04 are shown in Figure 4. We can draw the following conclusions: (1) The dimensionality of  $Z_E$  has limited influence on the experimental results, proving that contrastive learning is capable of achieving effective semantic alignment with relatively few parameters. (2) Appropriately increasing the batch size can improve the forecasting accuracy of STID. A larger batch size increases the number of negative data pairs, thereby enhancing the model’s robustness and its ability to capture semantics. However, the batch size that is too large can lead to underfitting issues. (3) Proper balance of temperature parameter is important to improve the effect of contrastive learning. Appropriately reducing the temperature parameter can improve the performance of STID and enhance its convergence. However,

**Table 4: Values of the corresponding hyperparameters.**

Methods	Config	Values
Merlin	weight of L1 Loss $\beta_1$	2
	weight of KD Loss $\beta_2$	2
	weight of CL Loss $\beta_3$	1
	temperature parameter	1
	dimensionality of $Z_E$	16
	batch size	16
STID	optimizer	Adam [24]
	learning rate	0.0002
	weight decay	0.0001
	embedding size	64
	node embedding size	64
	temporal embedding size (day)	64
MTGNN	temporal embedding size (week)	64
	number of layers	3
	dropout	0.15
	learning rate schedule	MultiStepLR
	clip gradient normalization	5
	milestone	[1,10,25,50,75,90,100]
Proposed	gamma	0.5
	epoch	101

**Figure 4: Results of hyperparameter experiments (PEMS04).**

setting the temperature parameter too small may lead to the problem of local optimality. (4) Among the three weights of the loss,  $\beta_1$  plays the most significant role. This is primarily because the knowledge distillation and contrastive loss are mainly used as constraints during the early training stages, whereas the model’s performance in the later stages primarily depends on the L1 loss.

## 4.6 Experiment on Multivariate Time Series Forecasting with Unfixed Missing Rates

To simulate the unfixed missing rates in real-world, we conduct the following experiments: (1) For the training and validation sets, we additionally process the data into four forms with missing rates of 25%, 50%, 75%, and 90%. (2) For the test set, we divide the time series into different segments based on time and randomly mask each segment with missing rates of 25%, 50%, 75%, and 90%. (3) For STID+Merlin, we train it as described in this paper: the unmasked data is used to train the teacher model, while the masked data is used to train the student model. Only the student model is used on the test set. (4) Baselines use three training ways: the first way involves training separate models for each missing rate, with the corresponding model selected for forecasting on the test set based on the current missing rate. The second way uses a single model trained on masked data with all four missing rates, which is directly tested on the test set. The final way trains a model using the unmasked data, which is directly tested on the test set.

Table 5 shows the results of several models on unfixed missing rates. The following conclusions can be drawn: (1) Trained only once, STID+Merlin achieves best results across all datasets. Experimental results demonstrate that STID+Merlin can effectively handle the unfixed missing rates. (2) For other baselines, training models separately for each missing rate performs better than training a single model for all missing rates, demonstrating that existing methods are limited in both practical value and robustness in MTSF with unfixed missing rates. (3) If a forecasting model is trained using only complete data, its forecasting performance significantly declines when data missing occurs. This demonstrates the poor robustness of existing models in real-world scenarios.

## 4.7 Efficiency

We compare the training times on the PEMS04 dataset for STID+Merlin, STID+GPT2, STID+GATGPT, iTransformer+TimesNet, and MTGNN+SPIN. Considering that STID+Merlin only needs to be trained once to adapt to different missing rates, whereas the other baselines require separate training sessions for each missing rate, we directly record the training time of the proposed STID+Merlin for a single epoch and sum up the training times for each missing rate for the other baselines. The experimental equipment is the  $8 \times$  RTX 4090 graphics card. Figure 5 displays the average training time per epoch for these models. Despite incorporating components such as contrastive learning and knowledge distillation during the training process, STID+Merlin also achieves satisfactory results in terms of efficiency. Besides, Since neither the imputation model nor the teacher model is needed during the inference phase, STID+Merlin offers greater efficiency advantages during inference.

## 5 Conclusion

This paper aims to enhance the robustness of existing forecasting models on MTSF with unfixed missing rates, which involves two main challenges: (1) missing values disrupting the semantics (global and local information) of MTS; (2) the missing rate is unfixed at different time periods in the real world. To this end, we propose Merlin based on offline knowledge distillation and multi-view contrastive learning. Merlin can assist existing models in effectively

**Table 5: Performance comparison results of several models on unfixed missing rates.**

Datasets	Methods	MAE	MAPE	RMSE
METR-LA	STID+Merlin	<b>3.41</b>	<b>10.27</b>	<b>7.08</b>
	STID+GATGPT (Separately)	3.48	10.74	7.31
	STID+GATGPT (Together)	3.55	10.87	7.48
	STID (Separately)	3.61	11.12	7.59
	STID (Together)	3.73	11.78	7.84
	STID (Complete)	4.06	13.62	8.91
	MTGNN+Merlin	<b>3.47</b>	<b>10.65</b>	<b>7.25</b>
	MTGNN+GATGPT (Separately)	3.53	10.85	7.44
	MTGNN+GATGPT (Together)	3.58	11.04	7.52
	MTGNN (Separately)	3.64	11.34	7.63
PEMS04	MTGNN (Together)	3.77	12.15	7.98
	MTGNN (Complete)	4.09	13.77	9.01
	STID+Merlin	<b>21.18</b>	<b>14.79</b>	<b>34.06</b>
	STID+GATGPT (Separately)	22.15	15.34	35.58
	STID+GATGPT (Together)	24.03	15.87	39.23
	STID (Separately)	24.52	16.44	39.97
	STID (Together)	25.64	17.66	41.43
	STID (Complete)	31.27	22.58	47.41
	MTGNN+Merlin	<b>22.34</b>	<b>15.08</b>	<b>35.94</b>
	MTGNN+GATGPT (Separately)	23.45	15.94	37.62

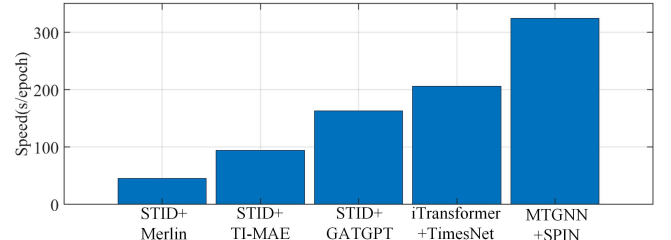


**Figure 5: Training time for each epoch of several models.**

achieving semantic alignment between incomplete observations with different missing rates and complete observations, thereby significantly enhancing their robustness to the unfixed missing rate. Extensive experiments show that the proposed model can achieve satisfactory forecasting results on all datasets and settings. Additionally, with the help of Merlin, existing forecasting models only need to be trained once to adapt to unfixed missing rates. In future work, we plan to investigate the effects of offline knowledge distillation when the teacher and student models utilize different neural network structures.

## Acknowledgments

This work is supported by NSFC No. 62372430, No. 62476264, and No. 62406312; the Postdoctoral Fellowship Program of CPSF under Grant Number GZC20241758 and BX20240385; the Youth Innovation Promotion Association CAS No.2023112; and HUA-Innovation fundings.

## References

- [1] Hyun Ahn, Kyunghee Sun, and Kwanghoon Pio Kim. 2022. Comparison of missing data imputation methods in time series forecasting. *Computers, Materials & Continua* 70, 1 (2022), 767–779.
- [2] Cristian Challu, Kin G Olivares, Boris N Oreshkin, Federico Garza Ramirez, Max Mergenthaler Canseco, and Artur Dubrawski. 2023. Nhits: Neural hierarchical interpolation for time series forecasting. In *Proceedings of the AAAI Conference on Artificial Intelligence*, Vol. 37. 6989–6997.
- [3] Jatin Chauhan, Aravindan Raghuvare, Rishi Saket, Jay Nandy, and Balaraman Ravindran. 2022. Multi-Variate Time Series Forecasting on Variable Subsets. In *Proceedings of the 28th ACM SIGKDD Conference on Knowledge Discovery and Data Mining*. 76–86.
- [4] Ling Chen, Donghui Chen, Zongjiang Shang, Binqing Wu, Cen Zheng, Bo Wen, and Wei Zhang. 2023. Multi-scale adaptive graph neural network for multivariate time series forecasting. *IEEE Transactions on Knowledge and Data Engineering* 35, 10 (2023), 10748–10761.
- [5] Si-An Chen, Chun-Liang Li, Sercan O Arik, Nathanael Christian Yoder, and Tomas Pfister. 2023. TSMixer: An All-MLP Architecture for Time Series Forecasting. *Transactions on Machine Learning Research* (2023). <https://openreview.net/forum?id=wbpXTuXgm0>
- [6] Ting Chen, Simon Kornblith, Mohammad Norouzi, and Geoffrey Hinton. 2020. A simple framework for contrastive learning of visual representations. In *International conference on machine learning*. PMLR, 1597–1607.
- [7] Xinyu Chen, Zhanhong Cheng, HanQin Cai, Nicolas Saunier, and Lijun Sun. 2024. Laplacian Convolutional Representation for Traffic Time Series Imputation. *IEEE Transactions on Knowledge and Data Engineering* 36, 11 (2024), 6490–6502.
- [8] Xiaodan Chen, Xiucheng Li, Bo Liu, and Zhijun Li. 2023. Biased Temporal Convolution Graph Network for Time Series Forecasting with Missing Values. In *The Twelfth International Conference on Learning Representations*.
- [9] Yakun Chen, Xianzhi Wang, and Guandong Xu. 2023. Gatgpt: A pre-trained large language model with graph attention network for spatiotemporal imputation. *arXiv preprint arXiv:2311.14332* (2023).
- [10] Fang Cheng and Hui Liu. 2024. Multi-step electric vehicles charging loads forecasting: An autoformer variant with feature extraction, frequency enhancement, and error correction blocks. *Applied Energy* 376 (2024), 124308.
- [11] Yu Chengqing, Yan Guangxi, Yu Chengming, Zhang Yu, and Mi Xiwei. 2023. A multi-factor driven spatiotemporal wind power prediction model based on ensemble deep graph attention reinforcement learning networks. *Energy* 263 (2023), 126034.
- [12] Andrea Cini, Ivan Marisca, and Cesare Alippi. 2022. Filling the G\_ap\_s: Multivariate Time Series Imputation by Graph Neural Networks. In *International Conference on Learning Representations*.
- [13] Jinliang Deng, Xiusi Chen, Zipei Fan, Renhe Jiang, Xuan Song, and Ivor W Tsang. 2021. The pulse of urban transport: Exploring the co-evolving pattern for spatiotemporal forecasting. *ACM Transactions on Knowledge Discovery from Data (TKDD)* 15, 6 (2021), 1–25.
- [14] Jinliang Deng, Xiusi Chen, Renhe Jiang, Xuan Song, and Ivor W Tsang. 2022. A multi-view multi-task learning framework for multi-variate time series forecasting. *IEEE Transactions on Knowledge and Data Engineering* 35, 8 (2022), 7665–7680.
- [15] Jinliang Deng, Xiusi Chen, Renhe Jiang, Du Yin, Yi Yang, Xuan Song, and Ivor W. Tsang. 2024. Disentangling Structured Components: Towards Adaptive, Interpretable and Scalable Time Series Forecasting. *IEEE Transactions on Knowledge and Data Engineering* 36, 8 (2024), 3783–3800.
- [16] Jiwen Deng, Renhe Jiang, Jiaqi Zhang, and Xuan Song. 2024. Multi-modality spatio-temporal forecasting via self-supervised learning. In *Proceedings of the Thirty-Third International Joint Conference on Artificial Intelligence*. 2018–2026.
- [17] Jinliang Deng, Feiyang Ye, Du Yin, Xuan Song, Ivor Tsang, and Hui Xiong. 2024. Parsimony or capability? decomposition delivers both in long-term time series forecasting. *Advances in Neural Information Processing Systems* 37 (2024), 66687–66712.
- [18] Aimee Dong, Jian Liu, Guodong Zhang, Zhonghe Wei, Yi Zhai, and Guohua Lv. 2023. Momentum contrast transformer for COVID-19 diagnosis with knowledge distillation. *Pattern Recognition* 143 (2023), 109732.
- [19] Jiaxiang Dong, Haixu Wu, Haoran Zhang, Li Zhang, Jianmin Wang, and Ming-sheng Long. 2024. Simmtm: A simple pre-training framework for masked time-series modeling. *Advances in Neural Information Processing Systems* 36 (2024).
- [20] Wenjie Du, David Côté, and Yanf Liu. 2023. Saits: Self-attention-based imputation for time series. *Expert Systems with Applications* 219 (2023), 119619.
- [21] Jianping Gou, Liyuan Sun, Baosheng Yu, Shaohua Wan, and Dacheng Tao. 2023. Hierarchical multi-attention transfer for knowledge distillation. *ACM Transactions on Multimedia Computing, Communications and Applications* 20, 2 (2023), 1–20.
- [22] Jincai Huang, Yongjun Xu, Qi Wang, Qi Cheems Wang, Xingxing Liang, Fei Wang, Zhao Zhang, Wei Wei, Boxuan Zhang, Libo Huang, et al. 2025. Foundation models and intelligent decision-making: Progress, challenges, and perspectives. *The Innovation* (2025), 100948.
- [23] Zhenhua Huang, Shunzhi Yang, MengChu Zhou, Zhetao Li, Zheng Gong, and Yunwen Chen. 2022. Feature map distillation of thin nets for low-resolution object recognition. *IEEE Transactions on Image Processing* 31 (2022), 1364–1379.
- [24] Diederik P Kingma and Jimmy Ba. 2014. Adam: A method for stochastic optimization. *arXiv preprint arXiv:1412.6980* (2014).
- [25] Mengzhang Li and Zhanxing Zhu. 2021. Spatial-temporal fusion graph neural networks for traffic flow forecasting. In *Proceedings of the AAAI conference on artificial intelligence*, Vol. 35. 4189–4196.
- [26] Yaguang Li, Rose Yu, Cyrus Shahabi, and Yan Liu. 2018. Diffusion Convolutional Recurrent Neural Network: Data-Driven Traffic Forecasting. In *International Conference on Learning Representations*.
- [27] Zhe Li, Zhongwen Rao, Lujia Pan, Pengyun Wang, and Zenglin Xu. 2023. Ti-mae: Self-supervised masked time series autoencoders. *arXiv preprint arXiv:2301.08871* (2023).
- [28] Ke Liang, Lingyuan Meng, Meng Liu, Yue Liu, Wenxuan Tu, Siwei Wang, Sihang Zhou, Xinwang Liu, Fuchun Sun, and Kunlun He. 2024. A survey of knowledge graph reasoning on graph types: Static, dynamic, and multi-modal. *IEEE Transactions on Pattern Analysis and Machine Intelligence* 46, 12 (2024), 9456–9478.
- [29] Hui Liu, Chengqing Yu, Haiping Wu, Zhu Duan, and Guangxi Yan. 2020. A new hybrid ensemble deep reinforcement learning model for wind speed short term forecasting. *Energy* 202 (2020), 117794.
- [30] Jiexi Liu and Songcan Chen. 2024. Timesurl: Self-supervised contrastive learning for universal time series representation learning. In *Proceedings of the AAAI Conference on Artificial Intelligence*, Vol. 38. 13918–13926.
- [31] Xinwei Liu, Muchuan Qin, Yue He, Xiwei Mi, and Chengqing Yu. 2021. A new multi-data-driven spatiotemporal PM<sub>2.5</sub> forecasting model based on an ensemble graph reinforcement learning convolutional network. *Atmospheric Pollution Research* 12, 10 (2021), 101197.
- [32] Yong Liu, Tengge Hu, Haoran Zhang, Haixu Wu, Shiyu Wang, Lintao Ma, and Mingsheng Long. 2024. iTransformer: Inverted Transformers Are Effective for Time Series Forecasting. In *The Twelfth International Conference on Learning Representations*. <https://openreview.net/forum?id=JefPAI8fah>
- [33] Ivan Marisca, Cesare Alippi, and Filippo Maria Bianchi. 2024. Graph-based Forecasting with Missing Data through Spatiotemporal Downsampling. In *Proceedings of the 41st International Conference on Machine Learning (Proceedings of Machine Learning Research)*, Vol. 235. PMLR, 34846–34865.
- [34] Ivan Marisca, Andrea Cini, and Cesare Alippi. 2022. Learning to reconstruct missing data from spatiotemporal graphs with sparse observations. *Advances in neural information processing systems* 35 (2022), 32069–32082.
- [35] Xiaoye Miao, Yangyang Wu, Jun Wang, Yunjun Gao, Xudong Mao, and Jianwei Yin. 2021. Generative semi-supervised learning for multivariate time series imputation. In *Proceedings of the AAAI conference on artificial intelligence*, Vol. 35. 8983–8991.
- [36] Alessio Monti, Angelo Porrello, Simone Calderara, Pasquale Coscia, Lamberto Ballan, and Rita Cucchiara. 2022. How many observations are enough? knowledge distillation for trajectory forecasting. In *Proceedings of the IEEE/CVF Conference on Computer Vision and Pattern Recognition*. 6553–6562.
- [37] Subhabrata Mukherjee and Ahmed Hassan Awadallah. 2020. XtremeDistil: Multi-stage Distillation for Massive Multilingual Models. In *Proceedings of the 58th Annual Meeting of the Association for Computational Linguistics*. 2221–2234.
- [38] Xiangfei Qiu, Jilin Hu, Lekui Zhou, Xingjian Wu, Junyang Du, Buang Zhang, Chenjuan Guo, Aoying Zhou, Christian S. Jensen, Zhenli Sheng, and Bin Yang. 2024. TFB: Towards Comprehensive and Fair Benchmarking of Time Series Forecasting Methods. *Proc. VLDB Endow.* 17, 9 (2024), 2363–2377.
- [39] Xiangfei Qiu, Zhe Li, Wanghui Qiu, Shiyan Hu, Lekui Zhou, Xingjian Wu, Zhengyu Li, Chenjuan Guo, Aoying Zhou, Zhenli Sheng, Jilin Hu, Christian S. Jensen, and Bin Yang. 2025. TAB: Unified Benchmarking of Time Series Anomaly Detection Methods. In *Proc. VLDB Endow.*
- [40] Xiangfei Qiu, Xingjian Wu, Yan Lin, Chenjuan Guo, Jilin Hu, and Bin Yang. 2025. DUEL: Dual Clustering Enhanced Multivariate Time Series Forecasting. In *SIGKDD*. 1185–1196.
- [41] Zezhi Shao, Tangwen Qian, Tao Sun, Fei Wang, and Yongjun Xu. 2025. Spatial-temporal large models: A super hub linking multiple scientific areas with artificial intelligence. *The Innovation* 6, 2 (2025), 100763.
- [42] Zezhi Shao, Fei Wang, Yongjun Xu, Wei Wei, Chengqing Yu, Zhao Zhang, Di Yao, Tao Sun, Guangyin Jin, Xin Cao, Gao Cong, Christian S. Jensen, and Xueqi Cheng. 2025. Exploring Progress in Multivariate Time Series Forecasting: Comprehensive Benchmarking and Heterogeneity Analysis. *IEEE Transactions on Knowledge and Data Engineering* 37, 1 (2025), 291–305.
- [43] Zezhi Shao, Zhao Zhang, Fei Wang, Wei Wei, and Yongjun Xu. 2022. Spatial-Temporal Identity: A Simple yet Effective Baseline for Multivariate Time Series Forecasting. In *Proceedings of the 31st ACM International Conference on Information and Knowledge Management*. 4454–4458.
- [44] Zezhi Shao, Zhao Zhang, Fei Wang, and Yongjun Xu. 2022. Pre-training enhanced spatial-temporal graph neural network for multivariate time series forecasting. In *Proceedings of the 28th ACM SIGKDD conference on knowledge discovery and data mining*. 1567–1577.
- [45] Zezhi Shao, Zhao Zhang, Wei Wei, Fei Wang, Yongjun Xu, Xin Cao, and Christian S. Jensen. 2022. Decoupled dynamic spatial-temporal graph neural network

for traffic forecasting. *Proceedings of the VLDB Endowment* 15, 11 (2022), 2733–2746.

[46] S Sridevi, S Rajaram, C Parthiban, S SibiArasan, and C Swadhikar. 2011. Imputation for the analysis of missing values and prediction of time series data. In *2011 international conference on recent trends in information Technology (ICRTIT)*. IEEE, 1158–1163.

[47] Jing Tan, Hui Liu, Yanfei Li, Shi Yin, and Chengqing Yu. 2022. A new ensemble spatio-temporal PM2.5 prediction method based on graph attention recursive networks and reinforcement learning. *Chaos, Solitons & Fractals* 162 (2022), 112405.

[48] Xianfeng Tang, Huaixiu Yao, Yiwei Sun, Charu Aggarwal, Prasenjit Mitra, and Suhang Wang. 2020. Joint modeling of local and global temporal dynamics for multivariate time series forecasting with missing values. In *Proceedings of the AAAI Conference on Artificial Intelligence*, Vol. 34. 5956–5963.

[49] Trang H Tran, Lam M Nguyen, Kyongmin Yeo, Nam Nguyen, Dzung Phan, Roman Vaculin, and Jayant Kalagnanam. 2023. An End-to-End Time Series Model for Simultaneous Imputation and Forecast. *arXiv preprint arXiv:2306.00778* (2023).

[50] Fei Wang, Di Yao, Yong Li, Tao Sun, and Zhao Zhang. 2023. AI-enhanced spatial-temporal data-mining technology: New chance for next-generation urban computing. *The Innovation* 4, 2 (2023).

[51] Kai Wang, Yu Liu, Qian Ma, and Quan Z Sheng. 2021. Mulde: Multi-teacher knowledge distillation for low-dimensional knowledge graph embeddings. In *Proceedings of the Web Conference 2021*. 1716–1726.

[52] Shiyu Wang, Haixiu Wu, Xiaoming Shi, Tengge Hu, Huakun Luo, Lintao Ma, James Y Zhang, and JUN ZHOU. 2024. TimeMixer: Decomposable Multiscale Mixing for Time Series Forecasting. In *International Conference on Learning Representations (ICLR)*.

[53] Gerald Woo, Chenghao Liu, Doyen Sahoo, Akshat Kumar, and Steven Hoi. 2021. CoST: Contrastive Learning of Disentangled Seasonal-Trend Representations for Time Series Forecasting. In *International Conference on Learning Representations*.

[54] Haixu Wu, Tengge Hu, Yong Liu, Hang Zhou, Jianmin Wang, and Mingsheng Long. 2023. TimesNet: Temporal 2D-Variation Modeling for General Time Series Analysis. In *The Eleventh International Conference on Learning Representations*.

[55] Haixu Wu, Hang Zhou, Mingsheng Long, and Jianmin Wang. 2023. Interpretable weather forecasting for worldwide stations with a unified deep model. *Nature Machine Intelligence* (2023), 1–10.

[56] Xingjian Wu, Xiangfei Qiu, Hongfan Gao, Jilin Hu, Chenjian Guo, and Bin Yang. 2025. K2VAE: A Koopman-Kalman Enhanced Variational AutoEncoder for Probabilistic Time Series Forecasting. In *ICML*.

[57] Zonghan Wu, Shirui Pan, Guodong Long, Jing Jiang, Xiaojun Chang, and Chengqi Zhang. 2020. Connecting the dots: Multivariate time series forecasting with graph neural networks. In *Proceedings of the 26th ACM SIGKDD international conference on knowledge discovery & data mining*. 753–763.

[58] Zonghan Wu, Shirui Pan, Guodong Long, Jing Jiang, and Chengqi Zhang. 2019. Graph wavenet for deep spatial-temporal graph modeling. In *Proceedings of the 28th International Joint Conference on Artificial Intelligence*. 1907–1913.

[59] Qing Xu, Zhenghua Chen, Mohamed Ragab, Chao Wang, Min Wu, and Xiaoli Li. 2022. Contrastive adversarial knowledge distillation for deep model compression in time-series regression tasks. *Neurocomputing* 485 (2022), 242–251.

[60] Yi Xu, Armin Bazarjani, Hyung-guun Chi, Chiho Choi, and Yun Fu. 2023. Uncovering the Missing Pattern: Unified Framework Towards Trajectory Imputation and Prediction. In *Proceedings of the IEEE/CVF Conference on Computer Vision and Pattern Recognition*. 9632–9643.

[61] Chuanguang Yang, Zhulin An, Linhang Cai, and Yongjun Xu. 2022. Mutual contrastive learning for visual representation learning. In *Proceedings of the AAAI Conference on Artificial Intelligence*, Vol. 36. 3045–3053.

[62] Chuanguang Yang, Zhulin An, Helong Zhou, Fuzhen Zhuang, Yongjun Xu, and Qian Zhang. 2023. Online knowledge distillation via mutual contrastive learning for visual recognition. *IEEE Transactions on Pattern Analysis and Machine Intelligence* 45, 8 (2023), 10212–10227.

[63] Chuanguang Yang, Helong Zhou, Zhulin An, Xue Jiang, Yongjun Xu, and Qian Zhang. 2022. Cross-image relational knowledge distillation for semantic segmentation. In *Proceedings of the IEEE/CVF Conference on Computer Vision and Pattern Recognition*. 12319–12328.

[64] Kun Yi, Qi Zhang, Wei Fan, Hui He, Liang Hu, Pengyang Wang, Ning An, Longbing Cao, and Zhendong Niu. 2023. FourierGNN: Rethinking Multivariate Time Series Forecasting from a Pure Graph Perspective. In *Thirty-seventh Conference on Neural Information Processing Systems*.

[65] Chengming Yu, Ji Qiao, Chao Chen, Chengqing Yu, and Xiwei Mi. 2024. TFE-former: A new temporal frequency ensemble transformer for day-ahead photovoltaic power prediction. *Journal of Cleaner Production* 448 (2024), 141690.

[66] Chengqing Yu, Fei Wang, Zezhi Shao, Tangwen Qian, Zhao Zhang, Wei Wei, Zhulin An, Qi Wang, and Yongjun Xu. 2025. GinAR+: A Robust End-To-End Framework for Multivariate Time Series Forecasting with Missing Values. *IEEE Transactions on Knowledge and Data Engineering* (2025), 1–14.

[67] Chengqing Yu, Fei Wang, Zezhi Shao, Tangwen Qian, Zhao Zhang, Wei Wei, and Yongjun Xu. 2024. Ginar: An end-to-end multivariate time series forecasting model suitable for variable missing. In *Proceedings of the 30th ACM SIGKDD Conference on Knowledge Discovery and Data Mining*. 3989–4000.

[68] Chengqing Yu, Fei Wang, Zezhi Shao, Tao Sun, Lin Wu, and Yongjun Xu. 2023. Dsformer: A double sampling transformer for multivariate time series long-term prediction. In *Proceedings of the 32nd ACM International Conference on Information and Knowledge Management*. 3062–3072.

[69] Chengqing Yu, Fei Wang, Yilun Wang, Zezhi Shao, Tao Sun, Di Yao, and Yongjun Xu. 2024. MGSSformer: A Multi-Granularity Spatiotemporal Fusion Transformer for Air Quality Prediction. *Information Fusion* (2024), 102607.

[70] Zhihan Yue, Yujing Wang, Juananyong Duan, Tianmeng Yang, Congrui Huang, Yunhai Tong, and Bixiong Xu. 2022. Ts2vec: Towards universal representation of time series. In *Proceedings of the AAAI Conference on Artificial Intelligence*, Vol. 36. 8980–8987.

[71] Xiaoxia Zhang, Shang Shi, HaiChao Sun, Degang Chen, Guoyin Wang, and Kesheng Wu. 2024. ACVAE: A novel self-adversarial variational auto-encoder combined with contrast learning for time series anomaly detection. *Neural Networks* 171 (2024), 383–395.

[72] Yunhao Zhang and Junchi Yan. 2022. Crossformer: Transformer utilizing cross-dimension dependency for multivariate time series forecasting. In *The Eleventh International Conference on Learning Representations*.

[73] Chuapan Zheng, Xiaoliang Fan, Cheng Wang, Jianzhong Qi, Chaochao Chen, and Longbiao Chen. 2023. INCREASE: Inductive Graph Representation Learning for Spatio-Temporal Kriging. In *Proceedings of the ACM Web Conference 2023*. 673–683.

[74] Tian Zhou, Peisong Niu, Liang Sun, Rong Jin, et al. 2023. One fits all: Power general time series analysis by pretrained lm. *Advances in neural information processing systems* 36 (2023), 43322–43355.

## A Compared with Different Loss Functions

In terms of constructing the loss function, this paper uses L1 Loss to evaluate the difference between the forecasting results of the student model and the ground truth. In addition, L2 Loss is used to evaluate the difference between the student model and the teacher model. To better analyze the impact of the loss function on the results, we consider using only one of the loss functions or swapping the use of the above two loss functions. Besides, considering that the KL-divergence is also commonly used to evaluate the similarity between different distributions, we use the KL divergence as a new loss function to replace hidden representation distillation and conducted experiments. Table 6 shows the MAE values of Merlin and other loss functions. The experimental results show that Merlin can get the best result. Additionally, compared to KL divergence, the MSE loss achieves better results. The main reason is that KL divergence focuses on improving the similarity between the distributions of representations, while MSE focuses on minimizing the numerical differences between representations. In summary, MTSF with missing values is a regression task, where minimizing numerical differences is more important.

## B Experiments When the Performance of the Teacher Model is Degraded

Both existing imputation models and our model assume that complete data can be collected during the training phase [7]. However, considering the possibility of incomplete data collection in real-world scenarios (i.e., missing values in the training set), the teacher model and imputation models might be trained on multivariate time series with missing values, potentially leading to degraded performance. Therefore, it is crucial to evaluate the effectiveness of Merlin under such conditions. In this section, we simulate scenarios where the training data for the teacher model has the 5% missing rate (this challenge also faced by imputation methods) and evaluate the improvements brought by Merlin and other imputation methods to different backbones under these conditions. Specifically, the

**Table 6: MAE values of the proposed method and other loss functions (The best results are shown in bold).**

Datasets	Methods	Missing rates			
		25%	50%	75%	90%
METR-LA	Proposed	<b>3.21</b>	<b>3.28</b>	<b>3.43</b>	<b>3.65</b>
	L1	3.23	3.31	3.44	3.67
	L2	3.28	3.37	3.53	3.73
	KL-divergence	3.26	3.34	3.49	3.71
	Swapping	3.27	3.35	3.51	3.72
Global Wind	Proposed	<b>5.76</b>	<b>5.85</b>	<b>5.97</b>	<b>6.08</b>
	L1	5.79	5.87	6.01	6.10
	L2	5.81	5.92	6.06	6.15
	KL-divergence	5.80	5.89	6.02	6.11
	Swapping	5.83	5.91	6.04	6.17

**Table 7: MAE values of Merlin and other methods (The missing rate of the training set is 5%).**

Backbone	Methods	METR-LA				Global Wind			
		25%	50%	75%	90%	25%	50%	75%	90%
STID	+Merlin	<b>3.25</b>	<b>3.33</b>	<b>3.46</b>	<b>3.69</b>	<b>5.80</b>	<b>5.88</b>	<b>6.01</b>	<b>6.11</b>
	+GATGPT	3.31	3.43	3.56	3.77	5.86	5.94	6.11	6.17
	+GPT2	3.34	3.48	3.59	3.80	5.88	5.97	6.16	6.24
	+TI-MAE	3.38	3.50	3.62	3.82	5.90	6.01	6.14	6.21
	+SPIN	3.30	3.49	3.64	3.83	5.85	5.98	6.15	6.26
	raw	3.44	3.57	3.79	3.96	5.95	6.09	6.18	6.30
DUET	+Merlin	<b>3.30</b>	<b>3.41</b>	<b>3.57</b>	<b>3.80</b>	<b>5.85</b>	<b>5.95</b>	<b>6.10</b>	<b>6.17</b>
	+GATGPT	3.32	3.48	3.60	3.86	5.87	5.98	6.12	6.20
	+GPT2	3.35	3.52	3.64	3.91	5.91	6.01	6.14	6.24
	+TI-MAE	3.35	3.49	3.59	3.86	5.90	6.02	6.15	6.25
	+SPIN	3.29	3.51	3.64	3.91	5.87	5.99	6.16	6.27
	raw	3.45	3.62	3.84	4.01	5.97	6.11	6.19	6.33
TimeMixer	+Merlin	<b>3.35</b>	<b>3.45</b>	<b>3.61</b>	<b>3.84</b>	<b>5.86</b>	<b>5.98</b>	<b>6.11</b>	<b>6.21</b>
	+GATGPT	3.39	3.52	3.67	3.90	5.90	6.03	6.15	6.24
	+GPT2	3.42	3.57	3.70	3.93	5.91	6.06	6.17	6.26
	+TI-MAE	3.45	3.59	3.74	3.98	5.94	6.08	6.16	6.27
	+SPIN	3.41	3.60	3.78	3.96	5.88	6.09	6.18	6.30
	raw	3.47	3.63	3.87	4.03	5.97	6.12	6.21	6.35
MTGNN	+Merlin	<b>3.27</b>	<b>3.39</b>	<b>3.54</b>	<b>3.77</b>	<b>5.84</b>	<b>5.97</b>	<b>6.07</b>	<b>6.15</b>
	+GATGPT	3.30	3.42	3.57	3.79	5.88	6.01	6.11	6.19
	+GPT2	3.34	3.47	3.64	3.89	5.91	6.03	6.15	6.23
	+TI-MAE	3.37	3.49	3.67	3.91	5.92	6.04	6.16	6.25
	+SPIN	3.31	3.45	3.59	3.84	5.87	5.98	6.13	6.22
	raw	3.43	3.58	3.81	3.95	5.96	6.10	6.20	6.34

original data is first modified to simulate the 5% missing rate. Subsequently, these datasets are further processed to simulate higher missing rates of 25%, 50%, 75%, and 90%. Merlin and baselines are trained on datasets with the 5% missing rate, as well as the datasets with subsequent missing rates of 25%, 50%, 75%, and 90%.

Table 7 shows the MAE values of Merlin and other methods. The following conclusions can be drawn: (1) Even when the data quality of the training sets for the teacher model decreases, Merlin can still effectively enhance the forecasting performance of several backbone models. (2) Compared to imputation models, Merlin demonstrates superior capability in restoring the forecasting performance of different backbones, further proving its practical value in real-world scenarios.

## C Compared with Multi-Stage Training

Considering that different training processes can affect the overall performance of the model, this section compares the effects of multi-stage training with adding all loss functions. The multi-stage training strategy used to construct the comparative experiment includes the following two aspects [37]: (1) Three-stage training: Firstly, train the model using the loss function of contrastive learning, then optimize the student model using the loss function of knowledge distillation, and finally optimize the student model using the L1 loss. (2) Two-stage training: Firstly, train the model using contrastive learning. Then optimize the student model using the combination of knowledge distillation and the L1 loss.

Table 8 shows the RMSE values of the proposed method and other multi-stage training methods. Experimental results show that compared with the multi-stage training strategy, the proposed method can achieve better forecasting results. The main reason is the problem of information forgetting in multi-stage training, which limits the performance of STID.

**Table 8: RMSE values of the proposed method and other multi-stage training methods (The best results are shown in bold).**

Datasets	Methods	Missing rates			
		25%	50%	75%	90%
METR-LA	Proposed	<b>6.64</b>	<b>6.78</b>	<b>7.18</b>	<b>7.64</b>
	Two-stage	6.67	6.83	7.25	7.67
	Three-stage	6.71	6.91	7.27	7.72
PEMS04	Proposed	<b>31.65</b>	<b>32.37</b>	<b>34.45</b>	<b>37.07</b>
	Two-stage	32.08	32.94	34.56	37.44
	Three-stage	32.34	33.06	34.82	37.61

## D Notations

Some commonly used notations are presented in Table 9.

**Table 9: Frequently used notation.**

Notation	size	Definitions
$N_H$	Constant	Length of historical observations
$N_L$	Constant	Length of forecasting results
$N_s$	Constant	Batch size
$N_v$	Constant	Number of variables
$N_c$	Constant	Number of features
$m$	Constant	Number of missing rates
$X$	$N_v \times N_H \times N_c$	Complete observations
$X_M$	$N_v \times N_H \times N_c$	incomplete observations
$Y$	$N_v \times N_L$	Forecasting results
FC	Functions	Fully connected layer
ReLU	Functions	Activation function ReLU
Mean	Functions	The mean of the Tensor
softmax	Functions	Activation function softmax